Estimation of Precipitation over India and Associated Oceanic Regions by Combined Use of Gauge and Multi-satellite Sensor Observations at Fine Scale

Anoop MISHRA[1*], Rakesh GAIROLA[2] and Akiyo YATAGAI[3]

[1]*Divecha Center for Climate Change, Indian Institute of Science, Bangalore, India*
[2]*Space Applications Centre, Indian Space Research Organization, India*
[3]*Faculty of Life and Environmental Science, University of Tsukuba, Japan*
**e-mail:anoopmishra_1@yahoo.co.in*

Abstract

The present study focuses on estimating rainfall (daily accumulated) using gauge and satellite observations over land and ocean regions of South Asia (30°S-50°N, 40°E-120°E) at a 0.25° × 0.25° spatial resolution for the period 2007-2010 (four years). The study utilizes observations from rain gauges, the Special Sensor Microwave/Imager (SSM/I) onboard the Defense Meteorological Satellite Program (DMSP), Precipitation Radar (PR) onboard the Tropical Rainfall Measuring Mission (TRMM) and geo-stationary satellite Meteosat from Eumetsat. The present study makes use of rainfall estimates by synergistic use of multi-satellite sensors using Meteosat Infrared and Water Vapor absorption channels and PR observations (Mishra *et al*., 2009b, 2010) and SSM/I-derived microwave estimates using a regional scattering index developed by Mishra *et al*., (2009a). The pixels over the land portion of the study area are filled with available rain gauge observations over the southern part (around 14°N and 78°E) of the study area, which has a dense network of Automatic Weather Station (AWS) rain gauges operated by the Indian Space Research Organization (ISRO). Pixels over the other part of the study area are filled with available microwave observations first, but if microwave observations are unavailable then these pixels are filled with microwave-calibrated infrared observations over the land and oceanic regions of the study area. The precipitation estimates from the present approach are validated against rain gauge observations and other available standard rainfall products like TRMM-3B42V6 and Global Precipitation Climatology Project (GPCP) version 2.1. The validation results show that the present approach of precipitation estimation is able to estimate rainfall with high accuracy.

Key words: precipitation, rain gauge, remote sensing, satellite, sensor

1. Introduction

Rainfall is a most unusual discontinuous atmospheric phenomena due to its high spatial and temporal variability. Accurate rainfall forecasts are essential for agricultural purposes. Furthermore, accurate assessment of rainfall is required in order for the total water budget of earth-atmosphere systems to be analyzed. The chief source of rainfall over South Asia is the monsoon, so a robust rainfall algorithm during pre-monsoon, monsoon and post-monsoon periods is required.

Over South Asia and its adjoining oceans, information from reliable ground-based radars and a dense network of rain gauges is available for limited areas. For overall synoptic applications, satellite-based estimates are highly desired. Standard estimations based on Infra Red (IR) measurements from satellites provide high temporal sampling. These estimates have large errors because IR radiances from cloud tops have only an indirect and weak relationship with surface rainfall. The most common Geostationary Operational Environment Satellite (GOES) Precipitation Index (GPI) technique (Arkin & Meisner, 1987), based on a simple infrared-brightness temperature (IR-TB) threshold algorithm, has been in operation to produce tropical and subtropical precipitation products on large temporal and spatial scales for climatological studies.

Satellite microwave measurements, on the other hand, have a strong physical relationship with rain and other hydrometeors but are at a disadvantage on temporal and spatial scales because of coarser spatial resolution, and lower orbiting satellites provide less coverage.

The development of hybrid techniques using the strengths of both microwave (MW) and IR, based on proper inter-calibration over the common areas of overlap is, therefore, highly desirable. Adler *et al*. (1994)

noted that opportunities exist to improve precipitation estimates by combining two types of data so that the strengths of each individual technique are maintained and their weaknesses are compensated for. Over the last few years, a number of groups have embarked on development of so-called hybrid techniques through synergistic use of multi-satellite sensor observations (Jobard & Desbois, 1994, Mishra *et al*., 2009a, 2010).

The present study focuses on estimating the rainfall over South Asia by combining rain gauge and merged satellite observations. The present technique's rainfall estimates were validated using Automatic Weather Station (AWS) rain gauges and other available rainfall products like Global Precipitation Climatology Project (GPCP) and TRMM-3B42.

2. Data Sources

The primary data used for this study were (1) infrared and water vapor observations from geo-stationary satellites and (2) microwave observations from the Tropical Rainfall Measuring Mission (TRMM) and the Defense Meteorological Satellite Program (DMSP), which are satellites in low earth orbits. The conventional data were obtained from AWS for validation purposes. Intercomparison of the estimates has been performed using available standard products like GPCP and TRMM-3B42V6.

2.1 Meteosat and TRMM satellite data

Meteosat is a geostationary earth observation satellite launched by the European Space Agency and now operated by the European Organization for the Exploration of Meteorological Satellites. It provides thermal infrared (TIR) and water vapor (WV) images at half-hourly intervals, with a spatial resolution of 4 km. In the present study, we utilized TIR and WV data from Meteosat-7.

The TRMM, launched in late November 1997 into a near-circular orbit, with 35° inclination from the equatorial plane, provides data using passive instruments in the optical and microwave spectra. It also carries a Precipitation Radar (PR). We used the surface rainfall data of Version-6 from Precipitation Radar (2A25) (Iguchi *et al*., 2000), along with Meteosat IR and WV for development of the algorithm, and a standard merged IR and MW data product called 3B42 (Huffman *et al.*, 2007) for the intercomparison.

2.2 Automatic Weather Station rain gauge data

AWS designed by the Indian Space Research Organization (ISRO) is a very compact, modular, rugged, powerful, low-cost system housed in a portable, self-contained package. Among many other sensors, it has a tipping bucket rain gauge with unlimited rain measuring capacity and an accuracy better than 1 mm. The data are relayed via satellite and are available at the website *www.mosdac.gov.in*. For the development and validation of the present algorithm, AWS rain gauge data during 2007, 2008, 2009 and 2010 were used. The AWS distribution over India is shown in Fig. 1.

2.3 GPCP Monthly data

The GPCP is an international project of the World Climate Research Programme Global Energy and Water Cycle Experiment, devoted to producing community analyses of global precipitation. In the present study, Version 2 GPCP monthly data (Adler *et al*., 2003) are used for a qualitative and quantitative comparison with the present technique.

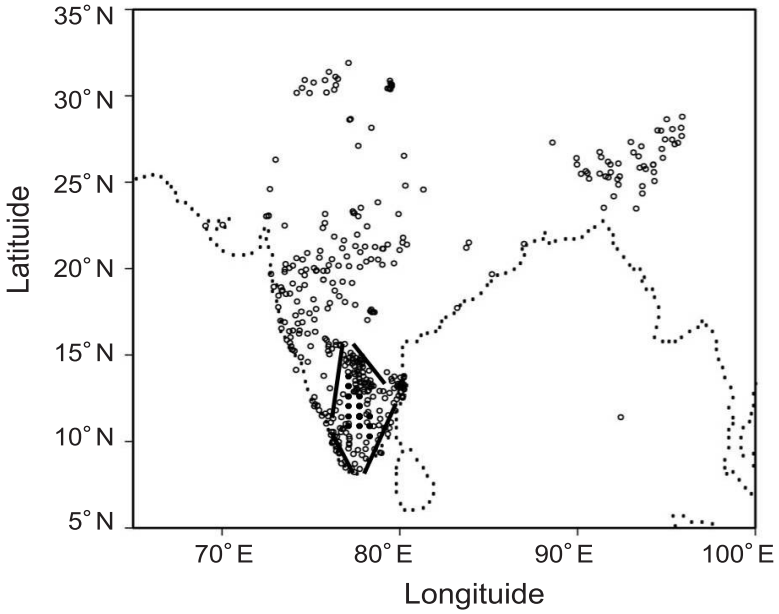

Fig. 1 ISRO AWS rain gauge distribution over the study area. Stations used in the algorithm development were located within the black bounded box**.**

2.4 SSM/I data

The Special Sensor Microwave/Imager (SSM/I) instrument was developed as part of the DMSP and was launched aboard the Air Force Block 5D polar- orbiting satellite on June 19, 1987. Built by Hughes Aircraft Company, the sensor uses four frequencies: 19.35, 22.235, 37.0, and 85.5 GHz. All frequencies except the water vapor absorption channel at 22.235 GHz are dual polarized. The resolution depends on the frequency and ranges from approximately 50 km for the 19 GHz channel to 15 km for the 85.5 GHz channel. For the present study the SSM/I (F13) data were used for the years 2007, 2008, 2009 and 2010.

3. Methodology

In the present study, rainfall over the study area was estimated by combining the rain gauge and satellite observations. The southern part (around 14°N and 78°E) of the study area has a dense network of ISRO AWS rain gauges (shown by the bounded box in Fig. 1). The density of the gauges is such that at least 2-6 gauges fall within each 0.25° × 0.25° box over most of the region. From this, spatially averaged rainfall estimates were constructed using a simple spatial averaging technique. If the number of gauges was less than 2 in any 0.25° × 0.25° box, then the pixels within the box were calibrated using weighted averaging by making use of the meteosat infrared brightness temperature, based on match-ups between the rain from the rain gauge and the meteosat brightness temperature. Thus, the rainfall over the southern part of the land portion of the study area was estimated using rain gauge observations.

Rainfall over the remaining part of the study area was estimated with SSM/I observations, using the regional scattering index technique (Mishra *et al*., 2009a) developed separately for the land and oceanic part of the study area. The technique is described below:

The procedure consists of two steps. In the first step, a region specific 'scattering index' (SI) is developed using a combination of the 19, 22 and 85 GHz channels separately for both land and oceanic regions. The second step establishes a new relationship between the scattering index and the rain rate using the TRMM PR data, mainly following Ferraro and Marks (1995).

For the development of the scattering index, the following relationship among 19, 22 and 85 GHz was established under non rainy conditions:

$$F=A+B\times Tv(19)+C\times Tv(22)+D\times (Tv(22))^2 \qquad (1)$$

where F is the brightness temperature of the 85 GHz channel and Tv(f) is the vertically polarized brightness temperature at frequency f. For land regions, the coefficients are A = 448.6809, B = –1.5456, C = –0.6020, and D = 0.0055. For oceanic regions, the coefficients are A = –362.4467, B = 1.1379, C = 3.5247, and D = –0.0078. After A, B, C and D are calculated, F is obtained, and the scattering index for the 85 GHz channel is defined as

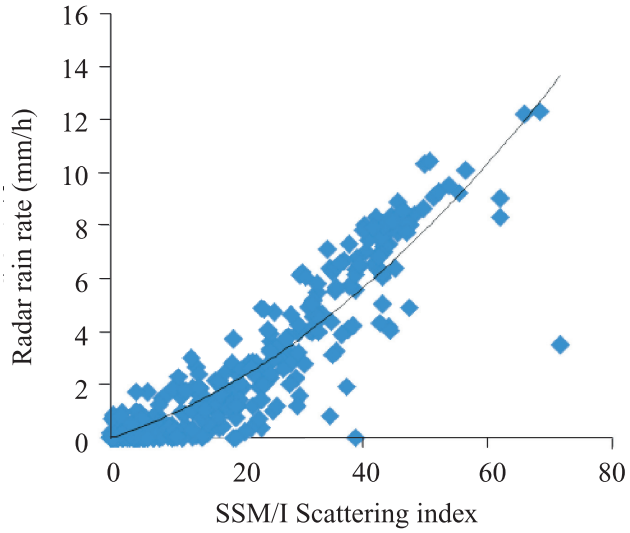

Fig. 2(a) Relationship between the scattering index from the SSM/I and rainfall from PR for the land portion of the study area. Line drawn over the scatters indicates the line of best fit.

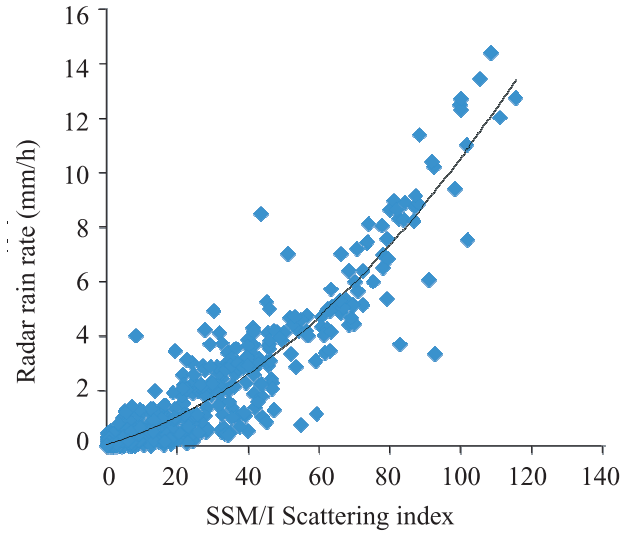

Fig. 2(b) Same as Fig. 2a, but for the oceanic region. Line drawn over the scatters indicates the line of best fit.

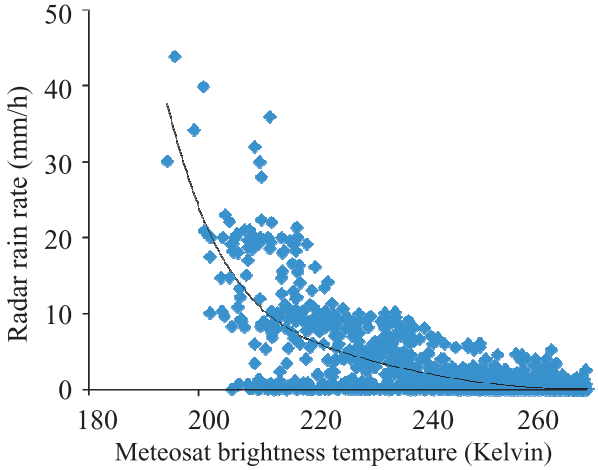

Fig. 2(c) Relationship between Meteosat brightness temperature and PR-rain rates.

$$SI\ (85) = F - Tv(85) \quad (2)$$

for the entire database (both raining and non-raining). From this step onwards, the index, SI, can be used to separate the scattering and non-scattering signals for a given set of independent data.

Now the SI has been calibrated with Precipitation Radar measurements. Specifically the following two relationships (Figs. 2a and 2b) were found to work best for the land and oceanic regions, respectively (Mishra *et al*., 2009a).

For land :

$$RR\ (mm/h) = .0268 \times (SI)^{1.5978} \quad (3)$$

For ocean:

$$RR\ (mm/h) = .0118 \times (SI)^{1.4985} \quad (4)$$

where RR is the rain rate in millimeters/hour.

The above two equations over land and ocean are applied to get the rainfall using the scattering index from SSM/I observations. Rainfall over coastal region is estimated by using Equation 2.

If the rain gauge and microwave observations are missing then the gap (both temporal and spatial) over the study area is filled in with microwave calibrated infrared observations obtained through synergistic use of multi-satellite sensor observations (Mishra *et al*., 2010). The scheme is as follows:

The procedure begins with a cloud classification scheme following Roca *et al*. (2002) from the Meteosat IR and WV channels to identify thin cirrus, deep convective and very deep convective clouds over each 0.25° × 0.25° grid box. Subsequently, calibration of IR brightness temperatures (IR-TBs) is performed (Fig. 2c) using PR rainfall within a 15 minute difference, in which the autocovariance function of rainfall decreases to approximately 0.9. Since TIR and PR measurements have nearly identical spatial resolution (4~5 km), non-uniformity is not considered on a finer scale. Finally the rainfall rates are computed based on the nonlinear power law relation between the collocated and near simultaneous IR-TBs and PR rainfall rates in each 0.25° × 0.25° grid box. After we applied both linear and non-linear regression between the TB and rainfall rate, we found that the following power-law regression equation best explains the relationship between the two variables (Mishra *et al*., 2010):

$$R = 16.6614 \times \exp(-(TB - 204.57)/16.52688) \quad (5)$$

In this way, the rainfall over vacant areas (where rain gauge and microwave observations are absent) is estimated by applying the above equation using Meteosat data.

4. Results and Discussion

The present technique has been developed by merging rain gauge, microwave and microwave-calibrated infrared observations. By utilizing the above technique, we created rainfall data sets for the period 2007 to 2010.

The usefulness of the technique can be examined by applying it to a recent cyclonic event. Only one case study is presented below for brevity.

For comparing the daily accumulated rainfall over a 0.25° × 0.25° box grid of the study area according to the present scheme with that from the TRMM-3B42V6, we have selected the case of a recent tropical cyclone named Laila, which developed on May 17, 2010 over the Bay of Bengal.

Figures 3a and 3b show the rainfall associated with the landfall of Tropical Cyclone Laila over the Andhra Pradesh coast on May 20, 2010, as observed by the pre-

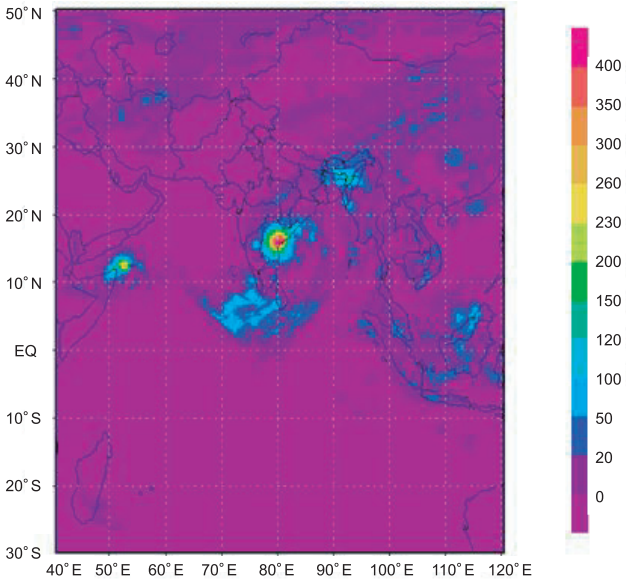

Fig. 3(a) 24-hour accumulated rainfall over a 0.25° × 0.25° grid using the present technique on May 20, 2010.

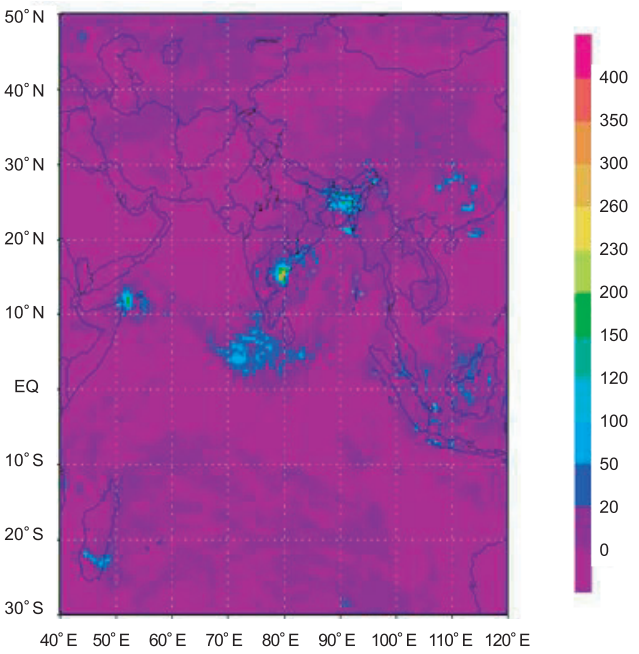

Fig. 3(b) 24-hour accumulated rainfall over a 0.25° × 0.25° grid using TRMM-3B42V6 on May 20, 2010.

sent technique and TRMM-3B42, respectively. From the above figures, one may confirm that the present scheme gives a reasonable depiction of the pattern and the intensity of the rain and it consistently matches those from TRMM-3B42V6 observations.

Further, for a quantitative assessment of the present scheme, we considered a total of 61,064 temporally and spatially collocated data points of daily accumulated rainfall during (1-5 July, 11-19 August and 12-14 December 2008; 12-17 September and 24-26 November 2009; and 17-21 May and 25-28 June 2010) from present technique and TRMM- 3B42V6 over the study area, with a grid of 0.25° × 0.25°.

Figure 4 shows the scatter plot and Table 1 shows the associated statistics between the two rainfall estimates. Rainfall obtained from the present technique and that from TRMM-3B42 V6 have a correlation coefficient of 0.86, with a root mean square error of 15.28, bias of 1.12, probability of detection (POD) of 0.72, false alarm ratio (FAR) of 0.25, and a skill score of 0.23. A description of FAR, POD and the skill score is given by Ebert & Manton (1998). From Fig. 4, we note a reasonable number of high rainfall points under the present scheme which are underestimated by the TRMM-3B42V6 observations. This may be due to the fact that TRMM-3B42V6 tends to underestimate orographic rain (Rahman *et al*., 2009), which may be depicted well by the present technique.

Further, in order to evaluate the performance of the present scheme we have compared it with GPCP observations. Figures 5a and 5b show a time series of the daily averaged monthly rainfall over central India (20-25°N and 76-82°E) with a 2.5° × 2.5° grid for the years 2007 and 2008, respectively, from the present scheme and GPCP observations. Both schemes are able to depict seasonal rainfall variation. They are able to detect the active and break cycle of the monsoon over central India during the southwest monsoon season. Both estimates consistently match each other, with the exception of a few high rainfall values during the monsoon season of 2007 from the present technique. This may again be due to the inability of the GPCP to capture high rainfall values associated with orography during the monsoon period (Rahman *et al*., 2009). Figure 6 shows the scatter plot of the rainfall from the present technique and those from the GPCP observations over the study area, with a 2.5° × 2.5° grid and Table 2 shows the associated statistics. For this purpose we considered 5,024 data points during January, June and September 2007; July and October 2008; and November and December 2009. It is

Table 1 Statistics comparing rainfall from present technique and that from TRMM-3B42V6.

No. of data points	61,064
Correlation coefficients	0.86
Root mean square error (mm)	15.28
Bias (mm)	1.12
TRMM-3B42 mean (mm)	10.68
Present scheme mean (mm)	11.80
Probability of detection (POD)	0.72
False alarm ratio (FAR)	0.25
Heidke skill score	0.23

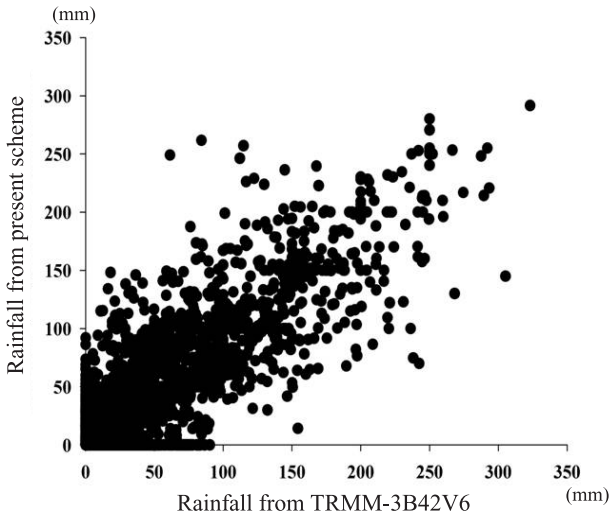

Fig. 4 Scatter plot between the TRMM-3B42V6 and present scheme daily rainfall over a 0.25° × 0.25° grid of the study area, *i.e.*, 30°S-50°N, 40°E-120°E.

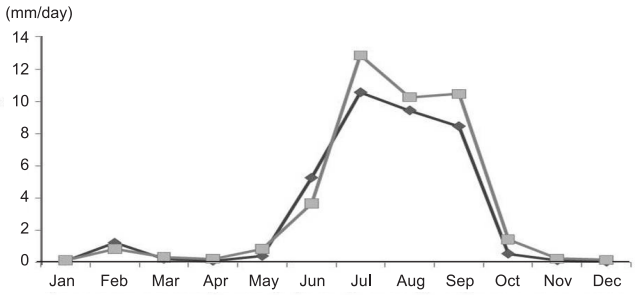

Fig. 5(a) Time series plot of daily average monthly rainfall over the Central Indian region (20-25° N and 76-82°E) over a 2.5° × 2.5° grid from the present scheme and GPCP data for the year 2007 over the study area, *i.e.*, 30°S-50°N, 40°E-120°E**.**

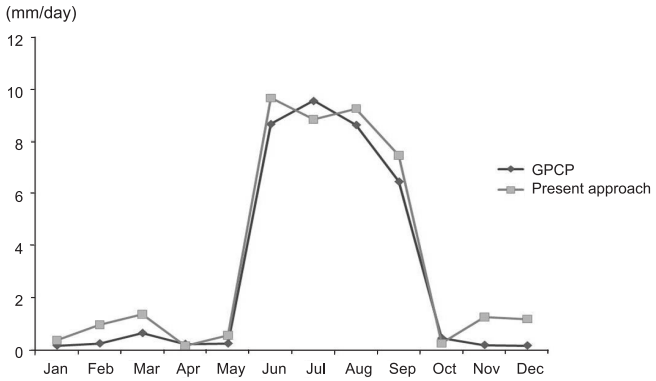

Fig. 5(b) Time series plot of daily average monthly rainfall over the Central Indian region (20-25° N and 76-82°E) over a 2.5° × 2.5° grid from the present scheme and GPCP data for the year 2008 over the study area, *i.e.*, 30°S-50°N, 40°E-120°E**.**

clear from the observations that rainfall from the present technique and that from the GPCP have a correlation coefficient of 0.89, root mean square error of 73.67, bias of 22.82, probability of detection (POD) of 0.78, false alarm ratio (FAR) of 0.19, and a skill score of 0.17. Again a few points with underestimated values of orographic rainfall from the GPCP are observed here. The GPCP product fails to show the observed high rainfall over the west coast of India, the northeast and Himalaya foothills. High rainfall over these regions, particularly over the Western Ghats and the Himalayan foothills is attributed to orography. These regions of high rainfall values are seen in the PR and SSM/I observations (Xie *et al*., 2006) and hence are observed under the present scheme also. From the statistics, it is clear that the present technique is able to retrieve rainfall with a very good accuracy.

Finally, the daily accumulated rainfall from the present scheme was validated against rain gauge observations over the India land region with a 0.25° × 0.25° grid. For this purpose we considered 1,371 spatially and temporally collocated data points from the present scheme and rain gauge observations during 17-25 June and 12-17 September 2007; 16-21 July, 7-11 August and 19-21 November 2008; and 1-5 March and 18-24 May 2009. Figure 7 shows the scatter plot and Table 3 presents the associated statistics. The two estimates in Fig. 7 have a correlation coefficient (R) of 0.77, rms error of 27.14 mm/day, bias of 2.71 mm/day, POD of 0.83, FAR of 0.34, and skill score of 0.29.

5. Summary and conclusions

The present study describes the development of a rainfall product for the period 2007-2010 over South Asia (30°S-50°N, 40°E-120°E) at a 0.25° × 0.25° spatial resolution (daily accumulated). The rain rates have been derived by merging rain gauge and multi-sensor satellite observations. Validation and statistical analyses have been performed using ground observations and other satellite rainfall products. Validation with rain gauges and comparison with other satellite products show that the present approach of rainfall estimation is able to estimate the rainfall over South Asia with high accuracy. There are several rainfall products available for research purposes, *e.g.*, water resources over Asia from the rain-gauge-based Asian Precipitation-Highly Resolved

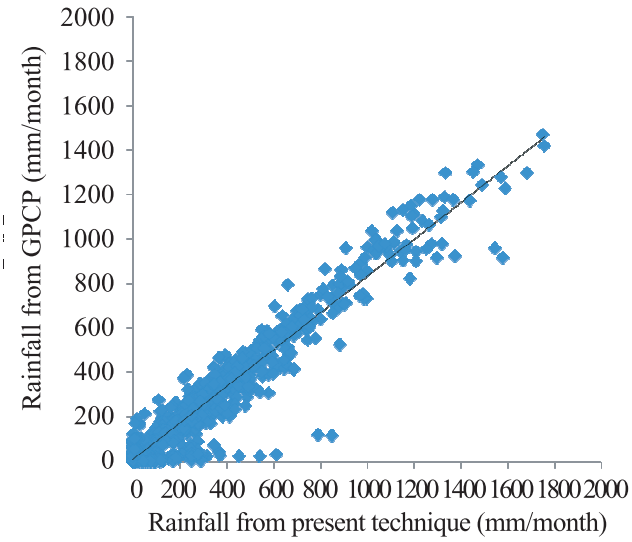

Fig. 6 Scatter plot between the monthly rainfall of GPCP and present scheme over a 2.5° × 2.5° grid of the study. Line drawn over scatters represents the line of best fit.

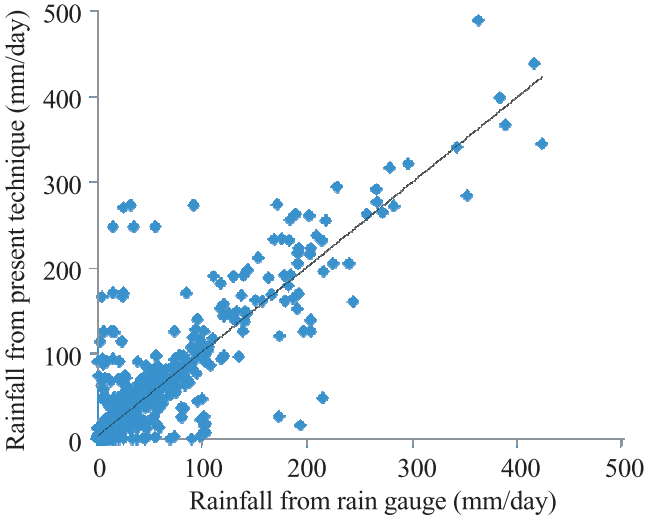

Fig. 7 Scatter plot between daily rainfall from rain gauge and present scheme over a 0.25° × 0.25° grid of the study. Line drawn over scatters represents the line of best fit.

Table 2 Statistics comparing rainfall from the present technique and that from GPCP.

No. of data points	5,024
Correlation coefficient	0.89
Root mean square error (mm)	73.67
Bias (mm)	22.82
GPCP mean (mm)	151.43
Present scheme mean (mm)	174.25
Probability of detection (POD)	0.78
False alarm ratio (FAR)	0.19
Heidke skill score	0.17

Table 3 Statistics comparing rainfall from present technique and that from rain gauge observations.

No. of data points	1371
Correlation coefficient	0.77
Root mean square error (mm)	27.14
Bias (mm)	2.71
Rain gauge mean (mm)	24.06
Present scheme mean (mm)	26.77
Probability of detection (POD)	0.83
False Alarm Ratio (FAR)	0.34
Heidke Skill Score	0.29

Observational Data Integration Towards Evaluation (APHRODITE) (Yatagai *et al*., 2009) and global rainfall products like TRMM-3B42 V6, GPCPV2, Climate Prediction Centre Morphing technique (CMORPH) (Joyce *et al*., 2004), and Global Satellite Mapping of Precipitation (GSMaP) (Kubota *et al*., 2007). The rain-gauge-based product does not provide information over the oceanic regions, while the above-mentioned other global rainfall products rely on rainfall estimation based on proxy variables like Polarization Corrected Temperatures (PCT) (Spencer *et al*., 1989), Scattering Indices (SI) (Ferraro & Marks, 1995), etc., which vary with the regions and seasons and do not perform well over South Asia (Mishra *et al*., 2009a); hence these rainfall products may not perform well over South Asian regions. The present rainfall product, based on rain-gauge and microwave observations using regional scattering indices and region-specific microwave-calibrated infrared observations developed for the South Asia region, is able to give very good estimates of rainfall over the land and oceanic portion of South Asia for research purposes.

Acknowledgement

This research was supported by the Environment Research and Technology Development Fund (A-0601) of the Ministry of the Environment, Japan. We thank the Ministry of the Environment of Japan for their funding through the Eco-Frontier Fellowship program (A06018). The TRMM-3B42V6, GPCP, SSM/I, AWS, and Meteosat data used in the present study are also thankfully acknowledged.

References

Adler, R.F, G.J Huffman and P.R. Keehn (1994) Global rain estimates from microwave adjusted geosynchronous IR data. *Remote Sensing Review*, 11: 125-135.

Adler, R.F., G.J. Huffman, A. Chang, R. Ferraro, P. Xie, J. Janowiak, B. Rudolf, U. Schneider, S. Curtis, D. Bolvin, A. Gruber, J. Susskind, P. Arkin and E., Nelkin (2003) The version 2 Global precipitation climatology project (GPCP) monthly precipitation analysis (1979-present). *Journal of Hydrometeorology*, 4: 1147-1167.

Arkin P.A. and B.N. Meisner (1987) The relationship between large scale convective rainfall and cold cloud cover over the western hemisphere during 1982-1984. *Monthly Weather Review,* 115: 51-74.

Ebert, E.E. and M.J. Manton (1998) Performance of satellite rainfall estimation algorithms during TOGA COARE. *Journal of Atmospheric Science*, 55: 1537-1557.

Ferraro, R.R. and G.F. Marks (1995) The development of SSM/I rain rate retrieval algorithms using ground based radar measurements. *Journal of Atmospheric and Oceanic Technology*, 12: 755-770.

Huffman, G. J., R.F. Adler, D.T. Bolvin, G. Gu, E.J. Nelkin, K.P. Bowman, Y. Hong, E.F. Stocker and D.B. Wolf (2007) The TRMM multisatellite precipitation analysis (TMPA): Quasi-global, multiyear, combined-sensor precipitation estimates at fine scales. *Journal of Hydrometeorology,* 8: 38-55.

Iguchi T, T. Kozu, R. Meneghini, J. Awaka and K. Okamoto (2000) Rain profiling algorithm for the TRMM Precipitation Radar. *Journal of Applied Meteorology*, 39 (12): 2038-2052.

Jobard I. and M. Desbois (1994) Satellite estimation of the tropical precipitation using the Meteosat and SSM/I data. *Atmospheric Research*, 34: 285-298.

Joyce R., J.E. Janowiak, P.A. Arkin and P. Xie (2004) CMORPH: A method that produces global precipitation estimates from passive microwave and infrared data at high spatial and temporal resolution. *Journal of Hydrometeorology,* 5: 487-503.

Mishra A., R.M. Gairola, A.K. Varma, Abhijit Sarkar and V.K. Agarwal (2009a) Rainfall Retrieval over Indian land and oceanic regions from SSM/I Microwave data. *Advances in Space Research*, 44: 815-823.

Mishra A., R.M. Gairola, A.K. Varma and V.K. Agarwal (2009b) Study of intense heavy rainfall events over India using KALPANA-IR and TRMM-precipitation radar observations, *Current Science*, 9, 5: 689-695.

Mishra A., R.M. Gairola, A.K. Varma and V.K. Agarwal (2010) Remote sensing of precipitation over Indian land and oceanic regions by synergistic use of multi-satellite sensors. *Journal of Geophysical Research*, 115: D08106, doi: 10.1029/2009 JD012157.

Rahman, S.H., D. Sengupta and M. Ravichandran (2009) Variability of Indian summer monsoon rainfall in daily data from gauge and satellite. *Journal of Geophysical Research,* 114: D17113, doi:10.1029/2008JD011694.

Roca, R., M. Viollier, L. Picon and M. Desbois (2002) A multisatellite analysis of deep convection and its moist environment over the Indian Ocean during the winter monsoon. *Journal of Geophysical Research*, 107: D19, 10.1029/2000JD000040.

Spencer R.W., H.M. Goodman and R.E. Hood (1989) Precipitation retrieval over land and ocean with the SSM/I: Identification and characteristics of the scattering signal. *Journal of Atmospheric and Oceanic Technology*, 6, 254-273.

T. Kubota, S. Shige, H. Hashizume, K. Aonashi, N. Takahashi, S. Seto, M. Hirose, Y.N. Takayabu, K. Nakagawa, K. Iwanami, T. Ushio, M. Kachi and K. Okamoto (2007) Global precipitation map using satellite-borne microwave radiometers by the GSMaP Project. *IEEE Transaction on Geoscience and Remote Sensing*, 45, 7: 2259-2275.

Xie, S. P., H. Xu, N.H. Saji and Y. Wang (2006) Role of narrow mountains in large-scale organization of Asian monsoon convection. *Journal of Climate*, 19: 3420-3429, doi:10.1175/ JCLI3777.1.

Yatagai, A., O. Arakawa, K. Kamiguchi, H. Kawamoto, M.I. Nodzu and A. Hamada (2009) A 44-year daily gridded precipitation dataset for Asia based on a dense network of rain gauges, *SOLA*, 5: 137-140, doi:10.2151/sola.2009-035.

Anoop Kumar MISHRA

Dr. Anoop Kumar MISHRA was born to Mrs Rani Mishra and Mr Mahesh Prasad Mishra on November 09, 1981 at Allahabad, Uttar Pradesh, India. After completing his M.Sc. from University of Allahabad in 2004, he joined Space Applications Centre, Indian Space Research Organization in 2006. He was awarded the PhD degree in Physics from Gujrat University, India in 2011. He worked as postdoctoral fellow at Research Institute for Humanity and Nature, Japan during June 2010 - March 2011. At present, he is working on precipitation retrieval using merged rain gauge and satellite observations at Centre for Atmospheric and Oceanic Science, Indian Institute of Science, India. He has developed rainfall retrieval techniques for the Indian land and oceanic regions using infrared, and microwave observations for the coming missions like INSAT-3D and Megha-Tropiques. He has worked on merged rainfall estimation technique using synergy from infrared and microwave observations.

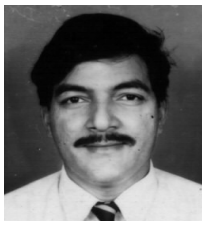

Rakesh Moham GAIROLA

Dr. Rakesh Moham GAIROLA, has been working with Space Applications Centre, Indian Space Research Organisation (ISRO) for the Radiative Transfer Modeling and Geophysical Parameter Retrievals and applications. He is currently involved in retrieval of rainfall from satellite microwave and optical sensors from various space based platforms, like Indo-French- Megha-Tropiques, TRMM and INSAT-3D etc. He has developed various operational algorithms for estimating rainfall at various spatial and temporal scales for different application purposes. Currently he is also working as the Principal Investigator of an AO-project under NASA-Global Precipitation Mission (GPM). He is also working as Associate Project Director and ISRO-Principal Investigator for an INDO-French (SARAL-Project). His other research interests are, Remote Sensing and its applications towards the global hydrologic cycle and Climate Change.

Akiyo YATAGAI

Dr. Akiyo YATAGAI is a climatologist and a researcher at the Faculty of Life and Environmental Sciences, University of Tsukuba. She received Doctor of Philosophy in 1996 from the Graduate School of Geoscience, University of Tsukuba. She was a Researcher at the Earth Observation Research Center, National Space Development Agency from 1995 to 2001. She was an Assistant Professor at the Research Institute for Humanity and Nature (RIHN), Kyoto from 2002 to 2011. She was a Principal Investigator of the Asian Precipitation – Highly Resolved Observational Data Integration Towards Evaluation of water resources (APHRODITE) project for 2006–2011, funded by the Global Environment Research Fund, Ministry of the Environment, Japan.

(Received 27 May 2011, Accepted 7 October 2011)